Int. J. Nonlinear Anal. Appl. 12 (2021) No. 1, 761-781
ISSN: 2008-6822 (electronic)
http://dx.doi.org/10.22075/ijnaa.2019.1543.1403

A simple, efficient and accurate new Lie-group shooting method for solving nonlinear boundary value problems

M. Hajiketabi, S. Abbasbandy*

Department of Applied Mathematics, Faculty of Science, Imam Khomeini International University, Qazvin 34149-16818, Iran

(Communicated by Madjid Eshaghi Gordji)

Abstract

The present paper provides a new method for numerical solution of nonlinear boundary value problems. This method is a combination of group preserving scheme (GPS) and a shooting–like technique which takes advantage of two powerful methods for solving nonlinear boundary value problems. This method is very effective to search unknown initial conditions. To demonstrate the computational efficiency, the mentioned method is implemented for some nonlinear exactly solvable differential equations including strongly nonlinear Bratu equation, nonlinear reaction–diffusion equation and one singular nonlinear boundary value problem. It is also applied successfully on two nonlinear three-point boundary value problems and a third-order nonlinear boundary value problem which the exact solutions of this problems are unknown. The examples show the power of method to search for unique solution or multiple solutions of nonlinear boundary value problems with high computational speed and high accuracy. In the test problem 5 a new branch of solutions is found which shows the power of the method to search for multiple solutions and indicates that the method is successful in cases where purely analytic methods are not.

Keywords: Group preserving scheme; Shooting method; Unique solution; Multiple solutions; Nonlinear boundary value problems.
2010 MSC: Primary 65L10; Secondary 76M60.

*Corresponding author
Email addresses: hajiketabi@edu.ikiu.ac.ir, mohammadhajiketabi@gmail.com (M. Hajiketabi), abbasbandy@ikiu.ac.ir (S. Abbasbandy)

Received: August 2016 *Revised:* October 2019

1. Introduction

Boundary value problems for ordinary differential equations play an fundamental role in both theory and applications. They are used to describe a large amount of physical, biological and chemical phenomena. Finding approximate solutions of nonlinear boundary value problems is very important in engineering. Nonlinear boundary value problems may have no, one or more than one solutions [1]-[4]. There are many methods to give approximate solutions of this problems, but despite the existence of multiple solutions for some of these problems, mentioned methods usually converge to only one branch of the solutions. It is important to predict the multiplicity of solutions and also approximate all branches of the solutions with good accuracy. In this paper we combine group preserving scheme (GPS) with shooting–like method for solving different types nonlinear boundary value problems and prediction the number of solutions, properties of solutions and compute the approximate solutions of this problems with high accuracy.
The GPS, which was first derived by Liu [5], uses the Cayley transformation and the Pade approximations in the augmented Minkowski space. The main difference between the GPS and the traditional numerical methods is that those schemes are all formulated directly in the usual Euclidean space $\mathbb{R}^n$, while the GPS is formulated in the Minkowski space $\mathbb{M}^{n+1}$. One direct advantage of the formulation in the augmented Minkowski space is that we can develop general group preserving schemes. This resulting schemes can avoid spurious solutions and ghost fixed points. The GPS approach has received a lot of attention in recent years. Hung–Chang Lee et al. [6] use from a modified GPS for solving the initial value problems of stiff ordinary differential equations. Chein–Shan Liu [7] studies the dynamic behavior of a single–mass, two degree of freedom bilinear oscillator, whose restoring force obeys a bilinear elastoplastic law, via GPS. Chein–Shan Liu [8] uses from GPS to solve backward heat conduction problems. Su–Ying Zhang et al. [9] combine GPS with RKMK methods for solving nonlinear dynamic system. Chein–Shan Liu [10] applies GPS on time–varying linear systems and Chein–Shan Liu [11] solves an inverse sturm–Liouville problem by a Lie–group method. S. Abbasbandy et al. [12] solve cauchy problem of the Laplace equation by GPS. Chein–Shan Liu et al. [13] combine the spring–damping regularization method (SDRM) and the mixed group–preserving scheme (MGPS) to solve highly ill–conditioned inverse Cauchy problem. Chein-Shan Liu et al [14] use a new form of this method for numerical differentiation of noisy signal. Chein–Shan Liu et al. [15] use another type of GPS to solve ordinary differential equations. S. Abbasbandy et al [16] use GPS for numerical simulation of periodic traveling wave solutions to the Casimir equation for the Ito system.
Liu [17] applied GPS for boundary value problems by search unknown initial condition through a weighting factor $r \in (0, 1)$. He called his method Lie–group shooting method (LGSM). This method is considered by authors; for example you can see [18]-[32]. In LGSM we require complex calculations for obtain unknown initial condition as a function respect to parameter $r \in (0, 1)$. In this calculations it is very important that we replace the originally un–equal boundary conditions by the boundary conditions with an equal value, that it's difficult for boundary value problems with nonlocal, nonlinear or three–point boundary conditions. Furthermore, the implementation of LGSM and perform the calculations for boundary value problems of higher two–order is difficult.

In this paper, we introduce a new method for solving boundary value problems. In this method we combine the GPS with a shooting method. We show the mention method is applicable for second–order of boundary value problems and higher order. Also, the method is suitable for boundary value problems with nonlocal, nonlinear or three–point boundary value problems. Since this method is combined with shooting method, we can predict the number of solutions by the number of best unknown initial condition that obtain from matching the right–end boundary condition. Therefore, this method is very suitable for nonlinear boundary value problems with multiple solutions. Ap-

plicability, Simplicity, high speed computation and high accuracy are important advantages of our method, that become apparent from different examples that we solve in section 4.

This paper is organized as follows. In section 2 we give a short sketch of the GPS for ODEs. In section 3 we combine GPS with shooting method for solving boundary value problems, also we explain the numerical method of obtain unknown initial condition by matching the right-end boundary. In section 4 we show applicability and high accuracy of method by various test problems.

2. Group preserving scheme

Liu [5] has derived a Lie group transformation for the augmented dynamical system on the future cone, and developed the group preserving scheme for an effective numerical solution of nonlinear ODEs. Consider a system of n ordinary differential equations:

$$\mathbf{u}'(x) = \mathbf{f}(\mathbf{u}(x), x), \quad \mathbf{u}(x) \in \mathbb{R}^n, \quad x \in \mathbb{R}, \tag{2.1}$$

where $\mathbf{u}(x)$ is an n-dimensional vector, x is an independent variable and $\mathbf{f}$ is a vector–valued function of $\mathbf{u}$ and x, also named vector field. We can transform Eq. (2.1) into the following $n+1$–dimensional augmented dynamical system:

$$\frac{d}{dx}\begin{bmatrix}\mathbf{u}\\ \|\mathbf{u}\|\end{bmatrix} = \begin{bmatrix}\mathbf{0}_{n\times n} & \dfrac{\mathbf{f}(\mathbf{u},x)}{\|\mathbf{u}\|}\\ \dfrac{\mathbf{f}^T(\mathbf{u},x)}{\|\mathbf{u}\|} & 0\end{bmatrix}\begin{bmatrix}\mathbf{u}\\ \|\mathbf{u}\|\end{bmatrix}. \tag{2.2}$$

Here we assume $\|u\| > 0$, and hence the above system is well–defined.

Obviously, the first equation in Eq. (2.2) is the same as the original Eq. (2.1), but the addition of the second equation gives us a Minkowskian structure of the augmented state variables of $\mathbf{U} = (\mathbf{u}^T, \|\mathbf{u}\|)^T$, satisfying the cone condition

$$\mathbf{U}^T\mathbf{g}\mathbf{U} = 0, \tag{2.3}$$

where

$$\mathbf{g} = \begin{bmatrix}\mathbf{I}_n & \mathbf{0}_{n\times 1}\\ \mathbf{0}_{1\times n} & -1\end{bmatrix}, \tag{2.4}$$

is a Minkowski metric, $\mathbf{I}_n$ is the identity matrix, and the superscript T stands for the transpose. In terms of $(\mathbf{u}, \|\mathbf{u}\|)$ Eq. (2.3) becomes

$$\mathbf{U}^T\mathbf{g}\mathbf{U} = \mathbf{u}\cdot\mathbf{u} - \|\mathbf{u}\|^2 = \|\mathbf{u}\|^2 - \|\mathbf{u}\|^2 = 0, \tag{2.5}$$

where the dot between two n–dimensional vectors denotes the Euclidean inner product. The cone condition is thus the most natural constraint that we can impose on the dynamical system (2.2). Consequently, we have a $n+1$–dimensional augmented system:

$$\mathbf{U}' = \mathbf{A}\mathbf{U}, \tag{2.6}$$

with a constraint (2.3), where

$$\mathbf{A} = \begin{bmatrix}\mathbf{0}_{n\times n} & \dfrac{\mathbf{f}(\mathbf{u},x)}{\|\mathbf{u}\|}\\ \dfrac{\mathbf{f}^T(\mathbf{u},x)}{\|\mathbf{u}\|} & 0\end{bmatrix}, \tag{2.7}$$

satisfying

$$\mathbf{A}^T\mathbf{g} + \mathbf{g}\mathbf{A} = \mathbf{0}, \tag{2.8}$$

is an element of the Lie algebra $\mathfrak{so}(n,1)$ of the proper orthochronous Lorentz group $\mathrm{SO}_0(n,1)$. Although the dimension of the new system is increased, Liu [5] has developed a group preserving scheme as follows to guarantee that each $\mathbf{U}_k$ can be located on the cone. The iteration proceeds as

$$\mathbf{U}_{k+1} = \mathbf{G}(k)\mathbf{U}_k, \tag{2.9}$$

where $\mathbf{U}_k$ denotes the numerical value of $\mathbf{U}$ at the discrete x_k, and $\mathbf{G}(k) \in \mathrm{SO}_0(n,1)$ satisfies

$$\mathbf{G}^T\mathbf{g}\mathbf{G} = \mathbf{g}, \tag{2.10}$$

$$\det \mathbf{G} = 1, \tag{2.11}$$

$$\mathrm{G}_0^0 > 0, \tag{2.12}$$

where $\mathrm{G}_0^0 > 0$ is the 00th component of $\mathbf{G}$.
With the integration of the Eq. (2.6) on interval $[x_k, x_{k+1}]$, we obtain:

$$\mathbf{U}_{k+1} = \exp\left[\int_{x_k}^{x_{k+1}} \mathbf{A}dx\right]\mathbf{U}_k \simeq \exp\left[\Delta x\mathbf{A}(k)\right]\mathbf{U}_k. \tag{2.13}$$

Since $\mathbf{A}(k) \in \mathfrak{so}(n,1)$, then $\exp\left[\Delta x\mathbf{A}(k)\right] \in \mathrm{SO}_0(n,1)$. An exponential mapping of $\mathbf{A}(k)$ admits the closed–form representation:

$$\exp[\Delta x\mathbf{A}(k)] = \begin{bmatrix} \mathbf{I}_n + \frac{(\alpha_k-1)}{\|\boldsymbol{f}_k\|^2}\boldsymbol{f}_k\boldsymbol{f}_k^T & \frac{\beta_k\boldsymbol{f}_k}{\|\boldsymbol{f}_k\|} \\ \frac{\beta_k\boldsymbol{f}_k^T}{\|\boldsymbol{f}_k\|} & \alpha_k \end{bmatrix} \tag{2.14}$$

where

$$\alpha_k = \cosh\left(\frac{\Delta x\|\mathbf{f}_k\|}{\|\mathbf{u}_k\|}\right), \tag{2.15}$$

$$\beta_k = \sinh\left(\frac{\Delta x\|\mathbf{f}_k\|}{\|\mathbf{u}_k\|}\right). \tag{2.16}$$

For notational convenience, we have used $\mathbf{f}_k = \mathbf{f}(\mathbf{u}_k, x_k)$. Substituting the above $\exp[\Delta x\mathbf{A}(k)]$ for $\mathbf{G}(k)$ into Eq. (2.9) , we obtain

$$\mathbf{u}_{k+1} = \mathbf{u}_k + \frac{(\alpha_k-1)\mathbf{f}_k.\mathbf{u}_k + \beta_k\|\mathbf{u}_k\|\|\mathbf{f}_k\|}{\|\mathbf{f}_k\|^2}\mathbf{f}_k = \mathbf{u}_k + \eta_k\mathbf{f}_k, \tag{2.17}$$

$$\|\mathbf{u}_{k+1}\| = \frac{\beta_k(\mathbf{f}_k\cdot\mathbf{u}_k) + a_k\|\mathbf{u}_k\|\|\mathbf{f}_k\|}{\|\mathbf{f}_k\|}. \tag{2.18}$$

This scheme therefore preserves group properties for all $\Delta x > 0$. In the practical numerical calculation, we only need Eq. (2.17) such that by knowing the initial value $\mathbf{u}_0$ we can obtain $\mathbf{u}_k, k = 1, 2, 3, \cdots$.

Theorem 1. The cone condition is preserved by Eqs. (2.17) and (2.18) for every time increment.
Proof . According to Eq. (2.5), we must prove

$$\mathbf{u}_{k+1}\cdot\mathbf{u}_{k+1} - \|\mathbf{u}_{k+1}\|^2 = 0. \tag{2.19}$$

From Eq. (2.17), we have

$$\mathbf{u}_{k+1}\cdot\mathbf{u}_{k+1}=\left(\mathbf{u}_k+\frac{(\alpha_k-1)\mathbf{f}_k.\mathbf{u}_k+\beta_k\|\mathbf{u}_k\|\|\mathbf{f}_k\|}{\|\mathbf{f}_k\|^2}\mathbf{f}_k\right)\cdot\left(\mathbf{u}_k+\frac{(\alpha_k-1)\mathbf{f}_k.\mathbf{u}_k+\beta_k\|\mathbf{u}_k\|\|\mathbf{f}_k\|}{\|\mathbf{f}_k\|^2}\mathbf{f}_k\right), \quad (2.20)$$

after doing the above inner product and possible simplifications, we obtain

$$\mathbf{u}_{k+1}\cdot\mathbf{u}_{k+1}=\frac{(1+\beta_k^2)\,\|\mathbf{u}_k\|^2\|\mathbf{f}_k\|^2+(\alpha_k^2-1)\,(\mathbf{f}_k\cdot\mathbf{u}_k)^2+2\alpha_k\beta_k(\mathbf{f}_k\cdot\mathbf{u}_k)\|\mathbf{u}_k\|\|\mathbf{f}_k\|}{\|\mathbf{f}_k\|^2}. \quad (2.21)$$

Therefore, according to definition α_k and β_k from Eqs. (2.15) and (2.16) we obtain

$$\mathbf{u}_{k+1}\cdot\mathbf{u}_{k+1}=\frac{\alpha_k^2\|\mathbf{u}_k\|^2\|\mathbf{f}_k\|^2+\beta_k^2(\mathbf{f}_k\cdot\mathbf{u}_k)^2+2\alpha_k\beta_k(\mathbf{f}_k\cdot\mathbf{u}_k)\|\mathbf{u}_k\|\|\mathbf{f}_k\|}{\|\mathbf{f}_k\|^2}=\frac{\Big(\alpha_k\|\mathbf{u}_k\|\|\mathbf{f}_k\|+\beta_k(\mathbf{f}_k\cdot\mathbf{u}_k)\Big)^2}{\|\mathbf{f}_k\|^2}=\|\mathbf{u}_{k+1}\|^2, \quad (2.22)$$

where the last equal is obtained from Eq. (2.18). Thus, the proof is finished. □

Theorem 2. Scheme (2.17), unconditionally preserves the fixed point and the property of the original differential equation.

Proof . First, we prove $\eta_k=\eta(x_k)>0$ for each x_k. From $\alpha_k>1$, $\forall\Delta x>0$ and $-\|\mathbf{f}_k\|\mathbf{u}_k\|\le\mathbf{f}_k\cdot\mathbf{u}_k\le\|\mathbf{f}_k\|\mathbf{u}_k\|$, we can prove that

$$\frac{\|\mathbf{u}_k\|}{\|\mathbf{f}_k\|}\left[\exp\left(\frac{\Delta x\|\mathbf{f}_k\|}{\|\mathbf{u}_k\|}\right)-1\right]\ge\eta_k\ge\frac{\|\mathbf{u}_k\|}{\|\mathbf{f}_k\|}\left[1-\exp\left(-\frac{\Delta x\|\mathbf{f}_k\|}{\|\mathbf{u}_k\|}\right)\right]>0,\quad\forall\Delta x>0. \quad (2.23)$$

Therefore, it is obvious that

$$\mathbf{u}_{k+1}=\mathbf{u}_k\Longleftrightarrow\mathbf{f}_k=\mathbf{0}. \quad (2.24)$$

This means that $\mathbf{u}_k$ is a fixed point of the discretized mapping (2.17) if and only if the point $\mathbf{u}_k$ is an equilibrium (critical, fixed) point of the system (2.1). We next investigate the property of the fixed point. The Jacobian of the map (2.17) is

$$J:=\frac{\partial\mathbf{u}_{k+1}}{\partial\mathbf{u}_k}=\mathbf{I}_n+\mathbf{f}_k\left(\frac{\partial\eta_k}{\partial\mathbf{u}_k}\right)^T+\eta_k\frac{\partial\mathbf{f}_k}{\partial\mathbf{u}_k}. \quad (2.25)$$

At the fixed point $\mathbf{f}_k=0$, we thus have

$$J=\mathbf{I}_n+\eta_k\frac{\partial\mathbf{f}_k}{\partial\mathbf{u}_k}. \quad (2.26)$$

Recalling that $\eta_k>0$, the property of the fixed point is not altered by the map (2.17). More precisely, the map (2.17) has the same type of stability that the system (2.1) has. □

According to the above two theorems, the long–term behavior of the original system can be described very well by this numerical scheme.

3. Combination of GPS and shooting method

In this section we combine the GPS with shooting method for solving nonlinear boundary value problems. Consider the following nonlinear boundary value problem of order two (the same trend is for higher order):

$$\begin{cases} u''(x) = f(x, u(x), u'(x)), \quad a \le x \le b, \\ u(a) = u_0, u(b) = u_f, \end{cases} \tag{3.1}$$

where the initial value u_0 and final value u_f are known. Using the change of variables $u(x) = u_1(x)$ and $u'(x) = u_2(x)$, we convert Eq. (3.1) to following vector form:

$$\begin{cases} \mathbf{u}'(x) = \mathbf{f}(x, \mathbf{u}(x)), \\ u_1(a) = u_0, u_1(b) = u_f, \end{cases} \tag{3.2}$$

where

$$\mathbf{u}(x) = \begin{bmatrix} u_1(x) \\ u_2(x) \end{bmatrix}, \quad \mathbf{f} = \begin{bmatrix} u_2(x) \\ f(x, u_1(x), u_2(x)) \end{bmatrix}. \tag{3.3}$$

Then, we transform boundary value problem (3.2) to following initial value problem:

$$\begin{cases} \mathbf{u}'(x) = \mathbf{f}(x, \mathbf{u}(x)), \\ u_1(a) = u_0, \\ u_2(a) = \alpha. \end{cases} \tag{3.4}$$

We will obtain α such that $|u_1^\alpha(b) - u_f| < \epsilon$ which ϵ is a certain small value. For this purpose, for a trial α, we solve initial value problem (3.4) by GPS from $x = a$ to $x = b$ and compare the end value of $u_1^\alpha(b)$ with the exact one $u_1(b) = u_f$. If $|u_1^\alpha(b) - u_f|$ is smaller than a given error tolerance ϵ, then the process of finding α is finished. Otherwise, we need to calculate the end values of $u_1(b)$ corresponding to different $\alpha_1 < \alpha$ and $\alpha_2 > \alpha$, which are denoted by $u_1^{\alpha_1}(b)$ and $u_1^{\alpha_2}(b)$, respectively. If $(u_1^{\alpha_1}(b) - u_f)(u_1^\alpha(b) - u_f) < 0$, there exists one root between $\alpha_1$and α. otherwise, the root is located between α and α_2. Then, we apply the half-interval method to find a suitable α. We will continue this process until find α such that $|u_1^\alpha(b) - u_f| < \epsilon$. In this process we require to calculate Eq. (3.4) by GPS at each of the calculation until $|u_1^\alpha(b) - u_f| < \epsilon$.

4. Numerical results

In this section we present the numerical results of new method on several nonlinear boundary value problems. Test problems 1, 2 and 3 have zero, one or two solutions according to value of parameters λ, m, ϕ and δ. The exact form solutions of this problems available. Comparison of numerical results obtained of our method with exact solutions of test problems 1, 2 and 3, we can conclude:

- The new method predict all branches of solutions very good.
- The new method approximate all branches of solutions with high accuracy.

But, for test problems 4, 5 and 6 only has been proved existence of solutions and some features of this solutions have also been reported. But, about the number of solutions and exact form of solutions we do not have accurate information. From solving examples 4, 5 and 6 by our numerical method we conclude:

- Numerical results obtained of our method have full agreement with the obtained analytical results.
- In some cases numerical results gives us more information about branches of solutions of problem.

4.1. Test problem 1

The Bratu problem is a nonlinear BVP that is used as a benchmark problem to test the accuracy of many numerical method [1, 2, 21, 33, 34]. The problem is given by

$$\begin{cases} u''(x) + \lambda e^{u(x)} = 0, \quad x \in [0,1], \\ u(0) = u(1) = 0, \end{cases} \tag{4.1}$$

where $\lambda > 0$. The Bratu problem has an analytical solution given in the following form [34]:

$$u(x) = -2\ln\left[\frac{\cosh\left((x-\frac{1}{2})\frac{\theta}{2}\right)}{\cosh(\frac{\theta}{4})}\right], \tag{4.2}$$

where θ is the solution of $\theta = \sqrt{2\lambda}\cosh(\frac{\theta}{4})$. The Bratu problem has zero, one or two solutions when $\lambda > \lambda_c$, $\lambda = \lambda_c$ or $\lambda < \lambda_c$ respectively, where the critical value λ_c satisfies the equation

$$1 = \frac{1}{4}\sqrt{2\lambda_c}\sinh\left(\frac{\theta_c}{4}\right). \tag{4.3}$$

It was evaluated that the critical value λ_c is given by $\lambda_c = 3.513830719$.
To apply the method, we firstly convert the boundary value problem (4.1) to equivalent initial value problem

$$\begin{cases} u''(x) + \lambda e^{u(x)} = 0, \quad x \in [0,1], \\ u(0) = 0, \\ u'(0) = \alpha. \end{cases} \tag{4.4}$$

Then we obtain α such that $|u(1) - 0| < \epsilon$ by the numerical method in section 3. We fix $\epsilon = 10^{-12}$ (this show the numerical result matches very well to the right–boundary condition) and the step-size $\Delta x = 0.0001$, and results have been given as follows for $\lambda = 2$, $\lambda = \lambda_c = 3.513830719$, $\lambda = 4$ and $\lambda = 5$. Figure (1) shows the Bratu equation has two solutions for $\lambda = 2$, unique solution for $\lambda = \lambda_c = 3.513830719$ and no solution for $\lambda = 4$ and 5, which has full agreement with the analytical concept of the critical value λ_c. Figure (2) shows exact and numerical dual solutions for $\lambda = 2$ and exact and numerical unique solution for $\lambda = \lambda_c = 3.513830719$. In Figure (3) we can show absolute error (in logarithmic scale) of dual solutions for $\lambda = 2$ for different Δx. Also, in Table (1) we show absolute error of unique solution for $\lambda = \lambda_c = 3.513830719$ for some different nodes. We show when the step size becomes smaller, numerical solutions convergence to exact solutions.

4.2. Test problem 2

A nonlinear model of diffusion and reaction in porous catalysts has been investigated by approximate analytical methods [1, 2, 35, 36, 37, 38]. In dimensionless variable the basic boundary value problem reads,

$$\begin{cases} u''(x) - \psi^2 u^m(x) = 0, \quad x \in [0,1], \\ u'(0) = 0, \quad u(1) = 1. \end{cases} \tag{4.5}$$

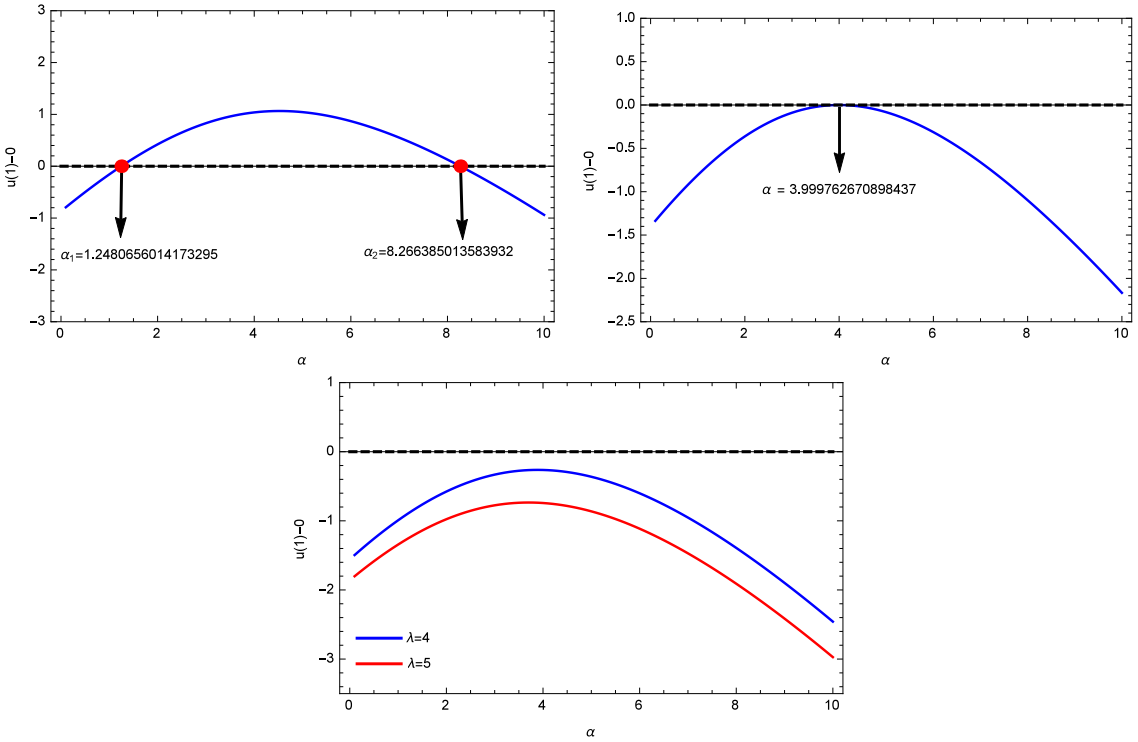

Figure 1: Plot of $u(1) - 0$ respect to α for $\lambda = 2$, $\lambda = \lambda_c = 3.513830719$ and $\lambda = 4, 5$ (respectively, from above left) for test problem 1.

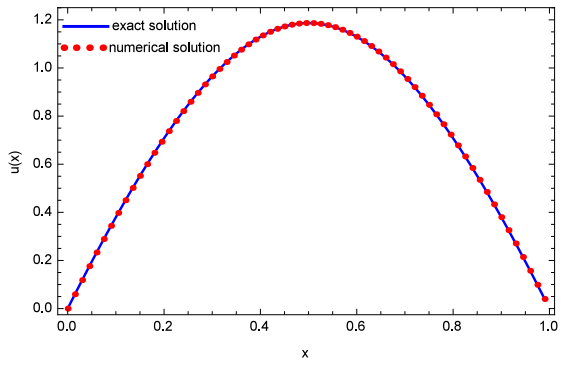

Figure 2: The comparison of numerical dual solutions of test problem 1 with the exact dual solutions for $\lambda = 2$ (left) and comparison of numerical unique solution of test problem 1 with the exact unique solution for $\lambda = \lambda_c = 3.513830719$ (right).

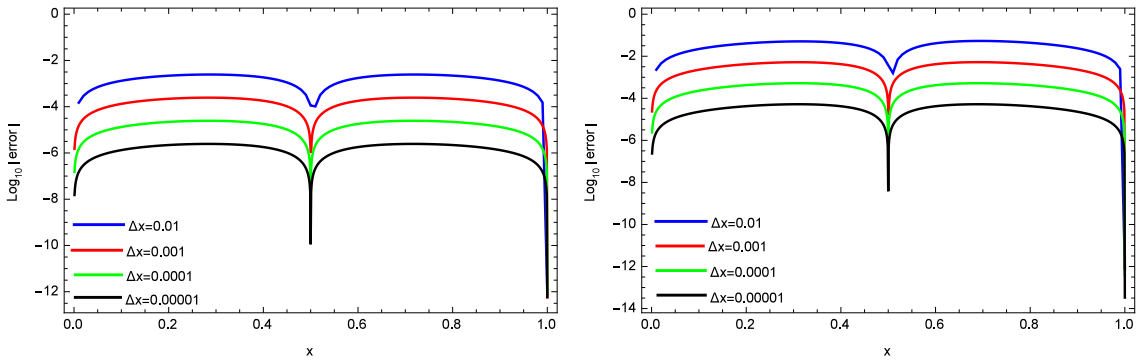

Figure 3: Absolute error (in logarithmic scale) of first branch (left) and second branch (right) for dual solutions of test problem 1 with $\lambda = 2$ for various Δx.

x	$\Delta x = 0.01$	$\Delta x = 0.001$	$\Delta x = 0.0001$	$\Delta x = 0.00001$
0	0	0	0	0
0.1	1.72932×10^{-3}	1.79683×10^{-4}	2.04852×10^{-5}	1.4759×10^{-6}
0.2	1.88855×10^{-3}	1.98756×10^{-4}	2.47392×10^{-5}	2.72026×10^{-6}
0.3	2.50284×10^{-4}	1.86987×10^{-5}	4.92517×10^{-6}	3.54441×10^{-7}
0.4	5.76176×10^{-3}	5.87503×10^{-4}	5.07901×10^{-5}	3.68798×10^{-6}
0.5	1.58693×10^{-2}	1.62084×10^{-3}	1.53847×10^{-4}	2.90846×10^{-5}
0.6	2.49998×10^{-2}	2.47907×10^{-3}	2.39603×10^{-4}	1.80027×10^{-5}
0.7	2.59347×10^{-2}	2.54113×10^{-3}	2.46867×10^{-4}	1.02705×10^{-5}
0.8	2.06147×10^{-2}	2.01179×10^{-3}	1.95932×10^{-4}	5.14020×10^{-5}
0.9	1.14139×10^{-2}	1.11215×10^{-3}	1.08483×10^{-4}	1.86488×10^{-5}
1	2.69139×10^{-13}	3.35075×10^{-13}	6.46312×10^{-13}	2.59323×10^{-13}

Table 1: Comparison of unique numerical solution of test problem 1 with unique exact solution for $\lambda = \lambda_c = 3.513830719$, in different number of nodal points for various Δx.

Magyari [36] have considered this model and given successfully exact analytical solutions in implicit form for all values of parameters of the problem. For the reaction order $m = -1$, the problem has dual solutions for $0 \leq \psi < \psi_{max}(m) = 0.765152$, for $\psi > \psi_{max}(m)$ no solution exist, and for $\psi = \psi_{max}(m)$ unique solution exists. In the range $-1 < m < 0$ of the reaction order, the problem has unique solution for $0 \leq \psi < \psi^*(m)$ and $\psi = \psi_{max}(m)$, two solutions for $\psi^*(m) \leq \psi < \psi_{max}(m)$ and for $\psi > \psi_{max}(m)$ no solution exist. For testing the numerical method we consider the problem when the model takes $m = -\frac{3}{4}$ for reaction order and $\psi = 0.2, 0.8, 0.9$ and $\psi = 1$. In this case, it was evaluated in [36] that the critical values $\psi^*(m)$ and $\psi_{max}(m)$, are given by $\psi^*(m) = 0.40$ and $\psi_{max}(m) = 0.839768$. It has been shown that the problem admit the following solution for $m = -\frac{3}{4}$,

$$x = \frac{2\sqrt{2}c_0^{\frac{7}{8}}}{35\psi}\sqrt{\left(\frac{u}{c_0}\right)^{\frac{1}{4}} - 1}\left[16 + 8\left(\frac{u}{c_0}\right)^{\frac{1}{4}} + 6\left(\frac{u}{c_0}\right)^{\frac{1}{2}} + 5\left(\frac{u}{c_0}\right)^{\frac{3}{4}}\right], \tag{4.6}$$

where if $\psi = 0.8$, $c_0 = 0.1836751649400644$ for first branch of solutions and $c_0 = 0.533047876754385$ for second branch of solutions. If $\psi = 0.2$, $c_0 = 0.9797428483877718$ for unique solution.
For apply the numerical method we convert the boundary value problem (4.5) to following initial

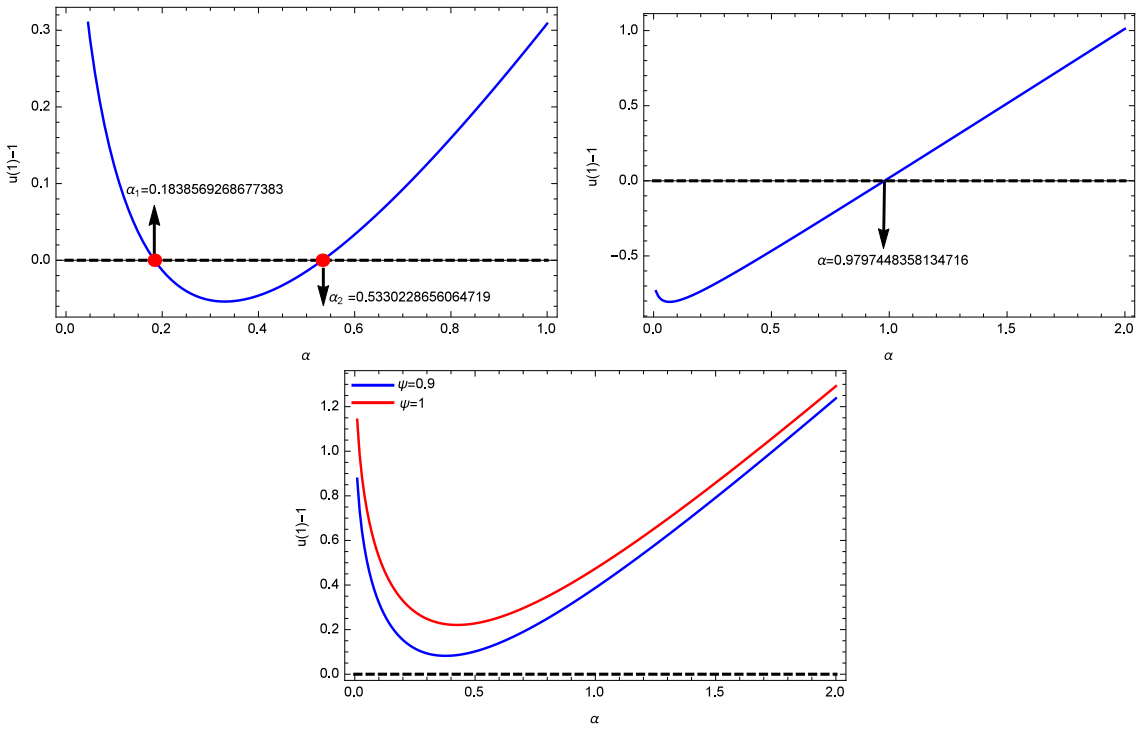

Figure 4: Plot of $u(1)-1$ for test problem 2 respect to α for $m=-\frac{3}{4}$ and $\psi=0.8$, $\psi=0.2$ and $\psi=0.9,1$ (respectively, from above left) for test problem 2.

value problem:

$$\begin{cases} u''(x)-\psi^2 u^m(x)=0, \quad x\in[0,1], \\ u(0)=\alpha, \\ u'(0)=0, \end{cases} \tag{4.7}$$

and obtain α such that $u(1)=1$. We fix $\epsilon=10^{-12}$ and the step-size $\Delta x=0.0001$ and results have been given as follows. Figure (4) shows the reaction-diffusion model has two solutions for $\psi=0.8$, unique solution for $\psi=0.2$ and no solution for $\psi=0.9,1$, which has full agreement with the analytical concept of the critical value $\psi^*(m)$ and $\psi_{max}(m)$ with reaction order $m=-\frac{3}{4}$. Figure (5) shows exact and numerical dual solutions for $\psi=0.8$ and exact and numerical unique solution for $\psi=0.2$. In Figure (6) we show absolute error (in logarithmic scale) of dual solutions for $\psi=0.8$ and for different Δx. Table (2) shows absolute error of unique solution for $\psi=0.2$ and for some different nodes. We can show when the step size becomes smaller, numerical solutions convergence to exact solutions.

4.3. Test problem 3

Let us consider the following BVP [41]

$$\begin{cases} u''(x)+\frac{1}{x}u'(x)=-\delta e^{u(x)}, \quad x\in(0,1), \\ u'(0)=0, \quad u(1)=0. \end{cases} \tag{4.8}$$

This problem is of the Robin type and is singular at the zero point $x=0$. The closed form solution of (4.8) is

$$u(x)=\ln\frac{8\rho}{\delta(1+\rho x^2)^2}, \tag{4.9}$$

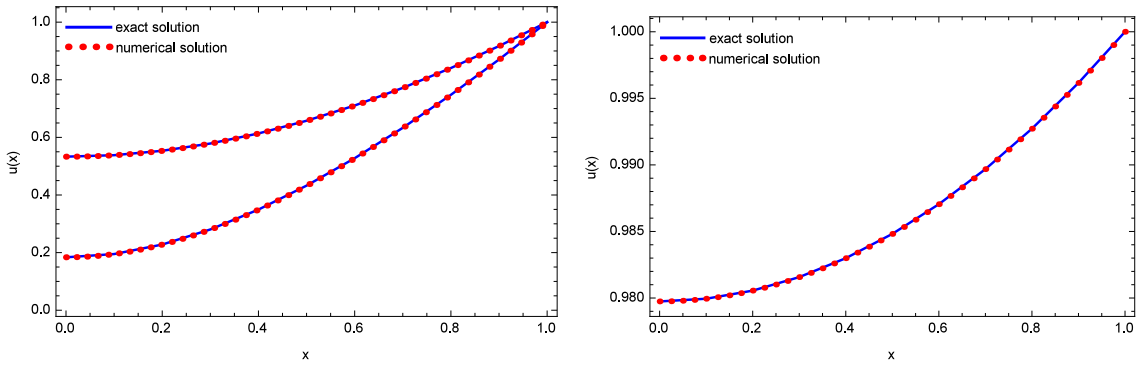

Figure 5: The comparison of numerical dual solutions of test problem 2 with the exact dual solutions for $m = -\frac{3}{4}$ and $\psi = 0.8$ (left), numerical unique solution of test problem 2 with the exact unique solution for $m = -\frac{3}{4}$, $\psi = 0.2$ (right).

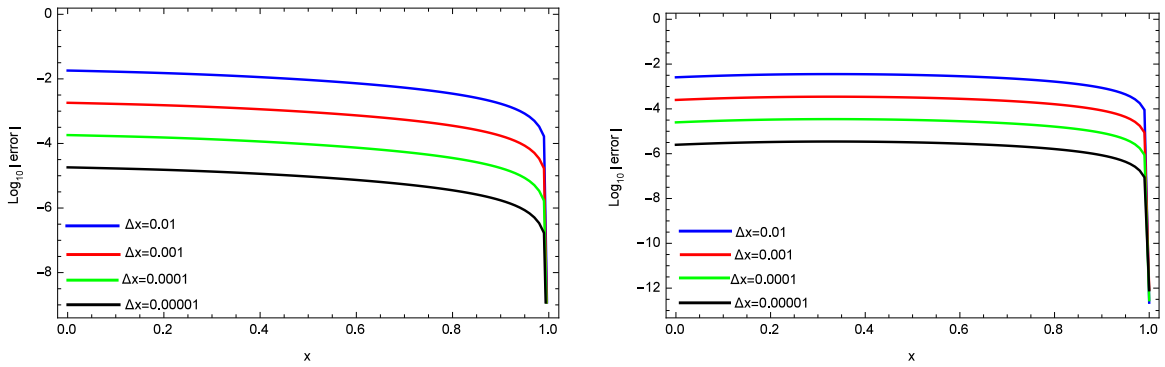

Figure 6: Absolute error (in logarithmic scale) of first branch (left) and second branch (right) for dual solutions of test problem 2 with $m = -\frac{3}{4}$ and $\psi = 0.8$ for various Δx.

x	$\Delta x = 0.01$	$\Delta x = 0.001$	$\Delta x = 0.0001$	$\Delta x = 0.00001$
0	1.98852×10^{-4}	1.98753×10^{-5}	1.98743×10^{-6}	1.98741×10^{-7}
0.1	1.78521×10^{-4}	1.79683×10^{-4}	1.78410×10^{-6}	1.78408×10^{-7}
0.2	1.58171×10^{-4}	1.98756×10^{-4}	1.58061×10^{-6}	1.58059×10^{-7}
0.3	1.37846×10^{-4}	1.86987×10^{-5}	1.37740×10^{-6}	1.37738×10^{-7}
0.4	1.17592×10^{-4}	5.87503×10^{-4}	1.17493×10^{-6}	1.17491×10^{-7}
0.5	9.74529×10^{-5}	1.62084×10^{-3}	9.73636×10^{-7}	9.73619×10^{-8}
0.6	7.74731×10^{-5}	2.47907×10^{-3}	7.73964×10^{-7}	7.73948×10^{-8}
0.7	5.76959×10^{-5}	2.54113×10^{-3}	5.76344×10^{-7}	5.76330×10^{-8}
0.8	3.81637×10^{-5}	2.01179×10^{-3}	3.81202×10^{-7}	3.81189×10^{-8}
0.9	1.89182×10^{-5}	1.11215×10^{-3}	1.88953×10^{-7}	1.88942×10^{-8}
1	2.55795×10^{-13}	3.35075×10^{-13}	3.07754×10^{-13}	8.69749×10^{-13}

Table 2: Comparison of unique numerical solution of test problem 2 with unique exact solution for $m = -\frac{3}{4}$ and $\psi = 0.2$, in different number of nodal points for various Δx.

where the integration constant ρ is determined by

$$\frac{8\rho}{\delta(1+\rho)^2} = 1. \tag{4.10}$$

It can be seen that for a given δ in the range of $0 < \delta < 2$, two distinct real roots of ρ Eq. (4.10) exist:

$$\rho = \frac{4 - \delta - 2\sqrt{2}\sqrt{2-\delta}}{\delta},$$
$$\rho = \frac{4 - \delta + 2\sqrt{2}\sqrt{2-\delta}}{\delta},$$

and correspondingly, there are two solutions for Eq. (4.8). For $\delta = 2$, there is only one solution corresponding to $\rho = 1$. This problem is singular in start point $x = 0$ and we can't apply GPS and thus our method. So, we consider $t = -x$ and solve following problem instead of Eq. (4.8)

$$\begin{cases} u''(t) - \frac{1}{-t}u'(t) = -\delta e^{u(t)}, \quad t \in (-1, 0), \\ u(-1) = 0, \quad u'(0) = 0. \end{cases} \tag{4.11}$$

Now, we transform boundary value problem (4.11) to following initial problem:

$$\begin{cases} u''(t) + \frac{1}{t}u'(t) = -\delta e^{u(t)}, \quad t \in (-1, 0), \\ u(-1) = 0, \\ u'(-1) = \alpha, \end{cases} \tag{4.12}$$

and apply our method and obtain α such that $|u'(0) - 0| < \epsilon$. If the target equation $|u'(0) - 0| < \epsilon$ is satisfied then we obtain the numerical solution of Eq. (4.8) by merely mapping the solution into the interval of $0 \le x \le 1$. We fix $\epsilon = 10^{-12}$ and the step-size $\Delta x = 0.0001$ and results have been given as follows for $\delta = 1, 2, 3$ and 4. Figure (7) shows Eq. (4.8) has two solutions for $\delta = 1$, unique solution for $\delta = 2$ and no solution for $\delta = 3$ and 4, which has full agreement with the analytical concept of the critical value δ. Figure (8) shows exact and numerical dual solutions for $\delta = 1$ and exact and numerical unique solution for $\delta = 2$. In Figure (9) we show absolute error (in logarithmic scale) of dual solutions for $\delta = 1$ and for different Δx. Table (3) shows absolute error of unique solution for $\delta = 2$ and for some different nodes.

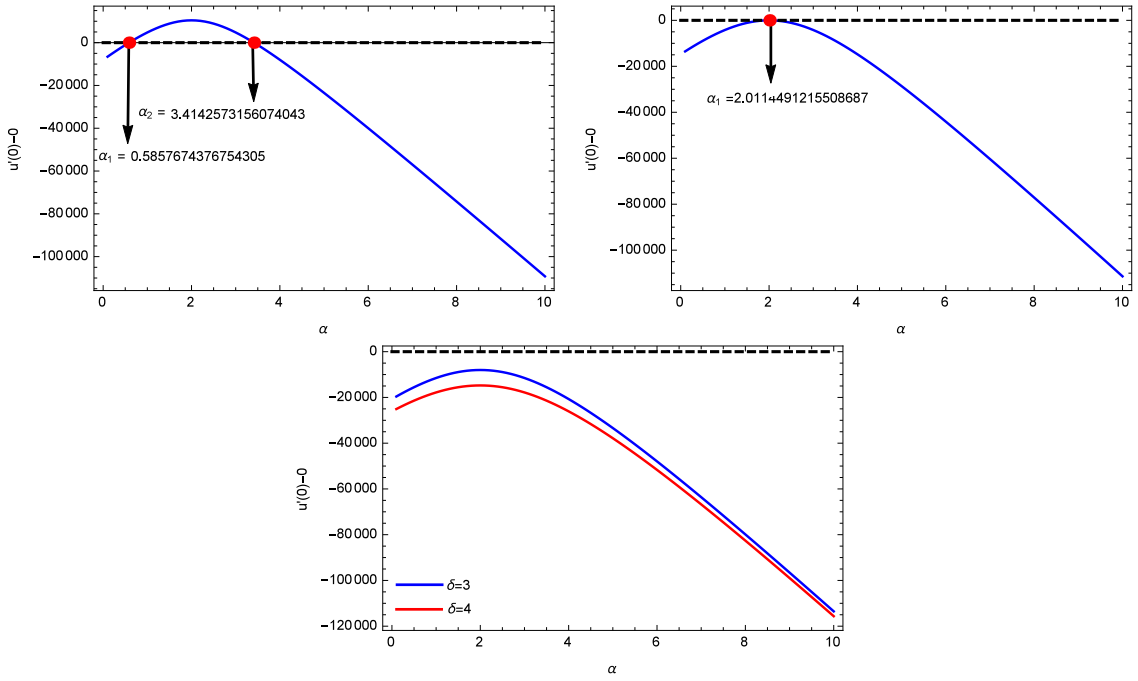

Figure 7: Plot of $u'(0) - 0$ for test problem 3 respect to α for $\delta = 1$, $\delta = 2$ and $\delta = 3, 4$ (respectively, from above left) for test problem 3.

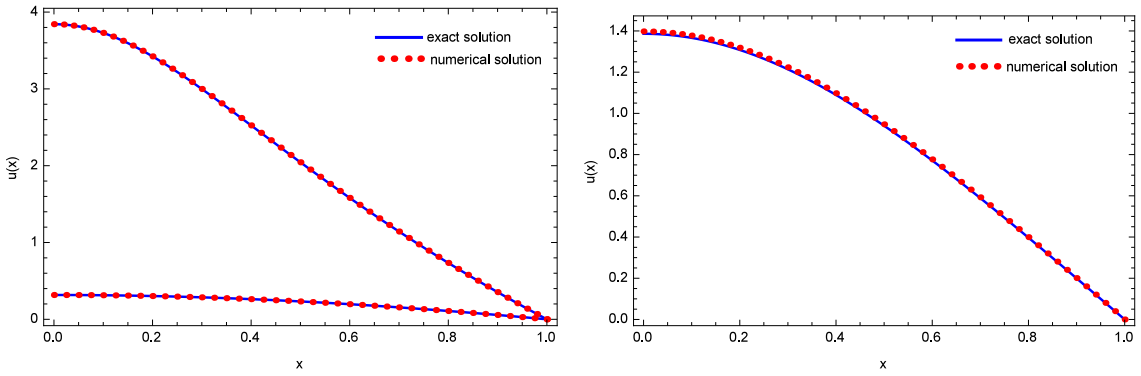

Figure 8: Comparison of numerical dual solutions of test problem 3 with exact dual solutions for $\delta = 1$ (left), numerical unique solution of test problem 3 with exact unique solution for $\delta = 2$ (right).

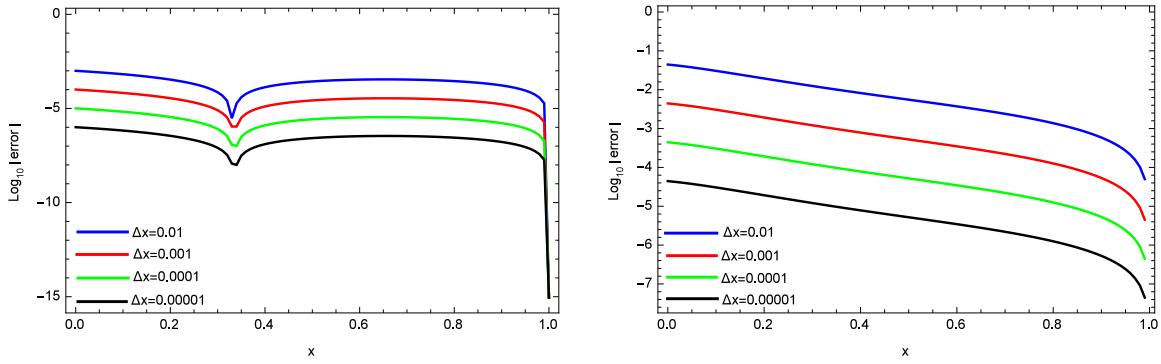

Figure 9: Absolute error (in logarithmic scale) of first branch (left) and second branch (right) for dual solutions of test problem 3 with $\delta = 1$ for various Δx.

x	$\Delta x = 0.01$	$\Delta x = 0.001$	$\Delta x = 0.0001$	$\Delta x = 0.00001$
0	1.31076×10^{-1}	3.77222×10^{-2}	1.15978×10^{-2}	3.63565×10^{-3}
0.1	1.26160×10^{-1}	3.67638×10^{-2}	1.13475×10^{-2}	3.56161×10^{-3}
0.2	1.16684×10^{-1}	3.44262×10^{-2}	1.06672×10^{-2}	3.35217×10^{-3}
0.3	1.03821×10^{-1}	3.09770×10^{-2}	9.63226×10^{-3}	3.03028×10^{-3}
0.4	8.87579×10^{-2}	2.67470×10^{-2}	8.34285×10^{-3}	2.62720×10^{-3}
0.5	7.26031×10^{-2}	2.20725×10^{-2}	6.90388×10^{-3}	2.17595×10^{-3}
0.6	5.62879×10^{-2}	1.72489×10^{-2}	5.40861×10^{-3}	1.70601×10^{-3}
0.7	4.05087×10^{-2}	1.25042×10^{-2}	3.92982×10^{-3}	1.24045×10^{-3}
0.8	2.57231×10^{-2}	7.99426×10^{-3}	2.51780×10^{-3}	7.95282×10^{-4}
0.9	1.21859×10^{-2}	3.81165×10^{-3}	1.20291×10^{-3}	3.80198×10^{-4}
1	0	0	0	0

Table 3: Comparison of unique numerical solution of test problem 3 with unique exact solution for $\delta = 2$, in different number of nodal points for various Δx.

4.4. Test problem 4

We consider nonlinear three–point boundary value problem

$$\begin{cases} u''(x) + \frac{3}{8}u(x) + \frac{2}{1089}(u'(x))^2 + 1 = 0, \quad x \in [0,1], \\ u(0) = 0, u(\frac{1}{3}) = u(1). \end{cases} \tag{4.13}$$

The uniqueness or multiplicity of solutions and the exact solutions are unknown, but the author in [39] gives some information. [39] proves the existence of one concave positive solution $u(x)$ such that $0 \leq max_{0\leq x\leq 1}|u(x)| \leq 4$ and $0 \leq max_{0\leq x\leq 1}|u'(x)| \leq 33$ and an iterative scheme for approximating this solution has been given. To apply our method we convert boundary value problem (4.13) to following initial value problem:

$$\begin{cases} u''(x) + \frac{3}{8}u(x) + \frac{2}{1089}(u'(x))^2 + 1 = 0, \quad x \in [0,1], \\ u(0) = 0, \\ u'(0) = \alpha, \end{cases} \tag{4.14}$$

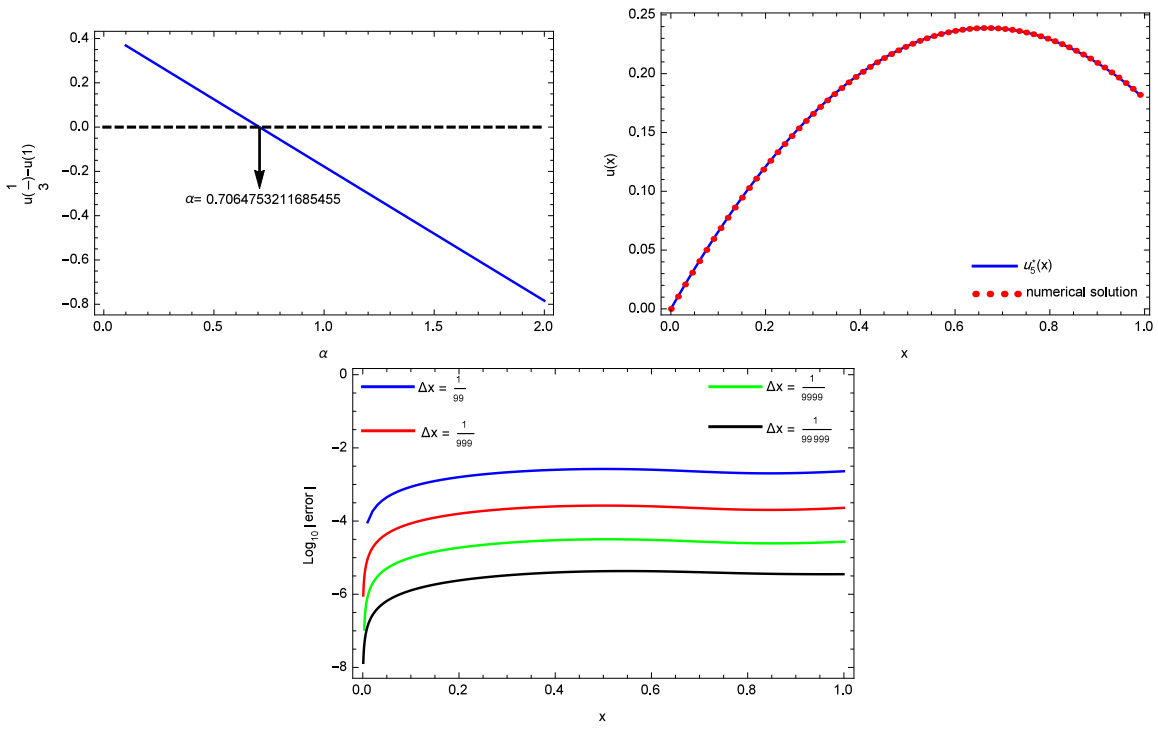

Figure 10: (Respectively, from above left, for test problem 4): plot of $u(\frac{1}{3})-u(1)$ respect to α, comparison of numerical solution and $u_5^*(x)$ (the fifth iteration of approximated solution in [39]), and absolute error (in logarithmic scale) for different Δx.

and obtain α such that $|u(\frac{1}{3}) - u(1)| < \epsilon$ by numerical method has been explained in section 3. For this purpose, we fix $\epsilon = 10^{-12}$ and the step–size $\Delta x = \frac{1}{9999}$ and results have been given as follows . Figure (10) shows the best α such that $|u(\frac{1}{3}) - u(1)| < \epsilon$ and as you can see we find one appropriate α with our method, which indicates this problem may has one solution. Comparison of solution obtained of our method and $u_5^*(x)$ (the fifth iteration of approximated solution in [39]) and absolute error (in logarithmic scale) for solution obtained of our method and $u_5^*(x)$, also can be seen in Figure (10). Table (4) shows absolute error in some different nodes for various Δx.

x	$\Delta x = 1/99$	$\Delta x = 1/999$	$\Delta x = 1/9999$	$\Delta x = 1/99999$
0	0	0	0	0
1/9	9.50592×10^{-4}	9.49553×10^{-5}	9.90512×10^{-6}	1.40518×10^{-6}
2/9	1.72804×10^{-3}	1.72595×10^{-4}	1.80494×10^{-5}	2.60476×10^{-6}
1/3	2.29761×10^{-3}	2.29426×10^{-4}	2.40581×10^{-5}	3.53556×10^{-6}
4/9	2.61049×10^{-3}	2.60565×10^{-4}	2.74208×10^{-5}	4.12457×10^{-6}
5/9	2.61567×10^{-3}	2.61015×10^{-4}	2.76225×10^{-5}	4.30345×10^{-6}
2/3	2.35000×10^{-3}	2.34811×10^{-4}	2.50592×10^{-5}	4.10128×10^{-6}
7/9	2.06914×10^{-3}	2.07368×10^{-4}	2.22676×10^{-5}	3.76808×10^{-6}
8/9	2.03747×10^{-3}	2.04199×10^{-4}	2.17933×10^{-5}	3.56193×10^{-6}
1	2.29761×10^{-3}	2.29426×10^{-4}	2.40581×10^{-5}	3.53556×10^{-6}

Table 4: Comparison of numerical results for test problem 4 with $u_5^*(x)$ (the fifth iteration of approximated solution in [39]), in different number of nodal points for various Δx.

4.5. Test problem 5

Consider the other three–point boundary value problem

$$\begin{cases} u''(x) + f(x, u(x), u'(x)) = 0, \quad 0 \le x \le 1, \\ u(0) = 0, \quad 2u(\frac{1}{3}) = u(1), \end{cases} \tag{4.15}$$

where

$$f\left(x, u(x), u'(x)\right) = \begin{cases} 9\sqrt{u(x)}, & 0 \le u(x) \le 36, \\ 180\sqrt{u(x) - 35.91} & 36 \le u(x) < +\infty. \end{cases}$$

This problem has been considered in [39] and the author proves the existence only two concave positive solutions u_1 and u_2 such that $\frac{3}{8} \le max_{0\le x\le 1}|u_1(x)| \le 36$ and

$$\frac{299.97}{2} \le max_{0\le x\le 1}|u_2(x)| \le 22535.91.$$

To apply numerical method we transform boundary value problem (4.15) to following initial value problem:

$$\begin{cases} u''(x) + f(x, u(x), u'(x)) = 0, \quad 0 \le x \le 1, \\ u(0) = 0, \\ u'(0) = \alpha. \end{cases} \tag{4.16}$$

Then, we obtain α such that $|2u(\frac{1}{3}) - u(1)| < \epsilon$. In Figure (11) we see the graph of $2u(\frac{1}{3}) - u(1)$ respect to α which shows the problem has three solutions corresponding to three roots $\alpha_1 = 33.78607764710614$, $\alpha_2 = 59.00776348389991$ and $\alpha_3 = 13392.584868312042$. The positive concave solutions corresponding to these roots are given in Figure (12) and we can see $\frac{3}{8} \le max_{0\le x\le 1}|u_1(x)| \le 36$ and $\frac{299.97}{2} \le max_{0\le x\le 1}|u_3(x)| \le 22535.91$ that Author in [39] shows the existence of two solutions with this two properties. In fact we show the multiplicity of solutions of (4.15) and find a new branch of solutions $u_2(x)$ such that $0 \le u_2(x) < 40$. So, results have full agreement with the obtained results in [39] and in addition gives us more information about branches of solutions.
This problem no have closed–form of exact or approximate solutions, for this reason we obtain RMS for residual error of this problem:

$$\sqrt{\frac{\sum_{i=1}^{n-1}\left(u''(x_i) - f(x_i, u(x_i), u'(x_i)\right)^2}{n-1}}, \tag{4.17}$$

where the values of $u(x_i)$ calculated from our method. Also we approximate $u''(x_i)$ with

$$\left(u'(x_{i+1}) - u'(x_{i-1})\right)/2\Delta x,$$

such that $u'(x_i)$ obtained by our method. Table (5) shows the RMS of residual error for two branches of solutions $u_1(x)$ and $u_2(x)$. We can show numerical results are good given that $u_1(x)$ and $u_2(x)$ are rapidly increasing in small interval $x \in [0, 1]$.

4.6. Test problem 6

We consider nonlinear third–order boundary value problem:

$$\begin{cases} u'''(x) + \frac{1}{2}\left(1 + \frac{1}{3}\left(u''(x)\right)^2\right)\left(1 + \frac{1}{3}u^2(x)\right) = 0, \quad x \in [0, 1], \\ u(0) = u(1) = 0, \quad u''(0) = 0. \end{cases} \tag{4.18}$$

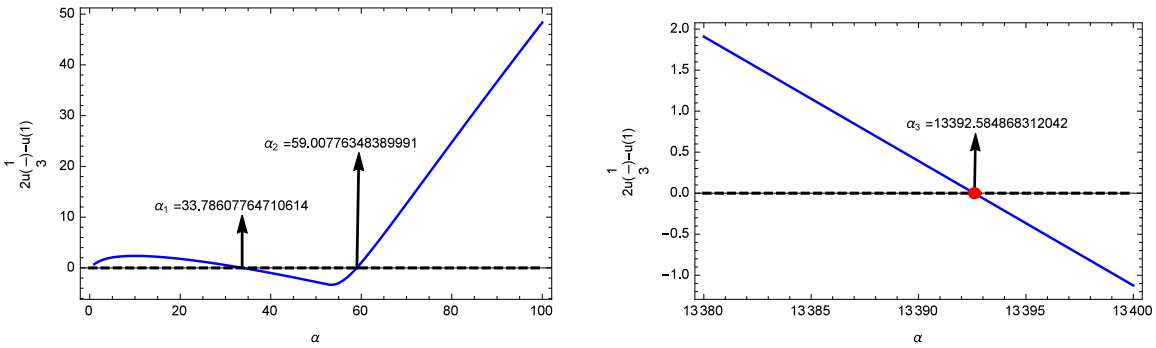

Figure 11: Plot of $2u(\frac{1}{3}) - u(1)$ respect to α for test problem 5.

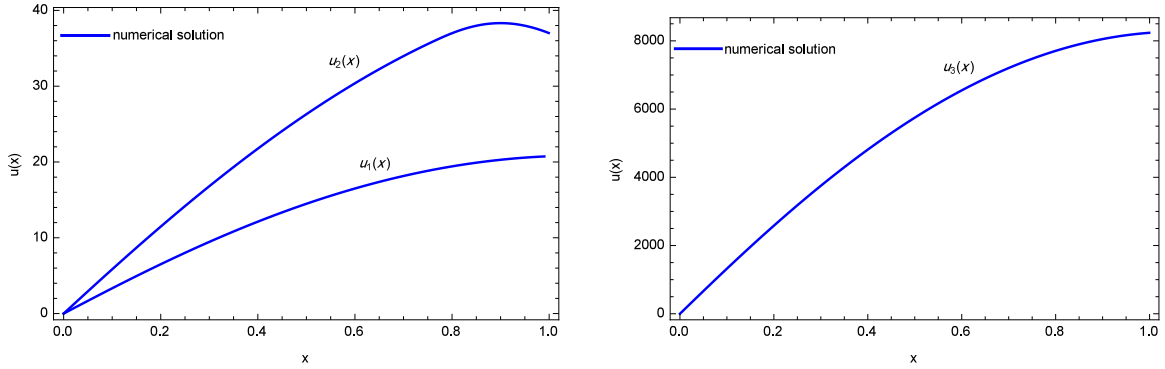

Figure 12: Plot of three branches of numerical solutions for test problem 5.

The branches of solutions	$\Delta x = 1/999$	$\Delta x = 1/9999$	$\Delta x = 1/99999$
$u_1(x)$	4.45682×10^{-2}	4.88086×10^{-3}	5.24924×10^{-4}
$u_2(x)$	5.15212×10^{-1}	5.16273×10^{-2}	5.17044×10^{-3}

Table 5: The RMS of residual error for two branches of test problem 5 for various Δx.

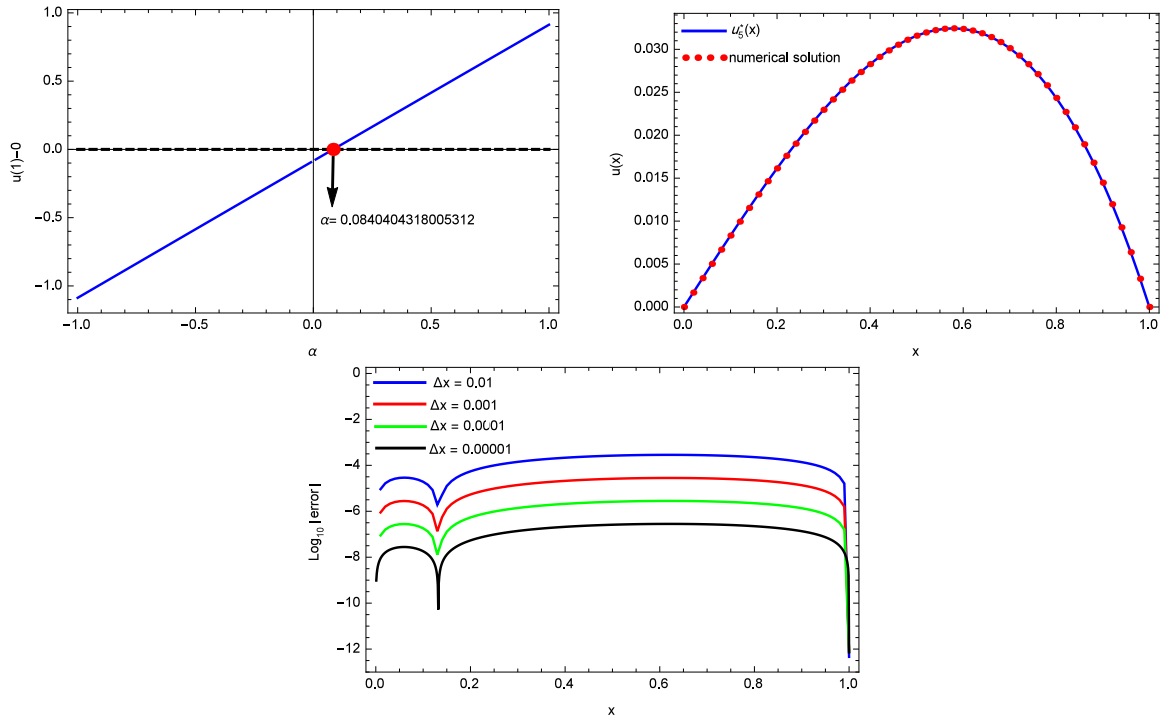

Figure 13: (Respectively, from above left, for test problem 6): plot of $2u(\frac{1}{3}) - u(1)$ respect to α, comparison of numerical solution with $u_5^*(x)$ (the fifth iteration of approximated solution in [40]), and absolute error (in logarithmic scale) for different Δx.

The uniqueness or multiplicity of solutions and the exact solutions are unknown, but the author in [40] gives some information. [40] proves the existence of one concave positive solution $u^*(x) \in \mathrm{C}^3[0,1]$ such that $0 \leq u^*(x) \leq 1$ and $-1 \leq (u^*(x))'' \leq 0$ for $0 \leq x \leq 1$ and an iterative scheme for approximating this solution has been given. To apply our method we convert boundary value problem (4.18) to following initial value problem:

$$\begin{cases} u'''(x) + \frac{1}{2}\left(1 + \frac{1}{3}\left(u''(x)\right)^2\right)\left(1 + \frac{1}{3}u^2(x)\right) = 0, \quad x \in [0,1], \\ u(0) = u''(0) = 0, \\ u'(0) = \alpha, \end{cases} \tag{4.19}$$

and obtain α such that $|u(1) - 0| < \epsilon$. Figure (13) shows the best α such that $|u(1) - 0| < 10^{-12}$, comparison of solution obtained of our method and $u_5^*(x)$ (the fifth iteration of approximated solution in [40]) and absolute error (in logarithmic scale) for solution obtained of our method and $u_5^*(x)$. For this problem we find only one α such that $|u(1) - 0| < 10^{-12}$, therefore this problem may has unique solution. Table (6) shows absolute error in some different nodes for various Δx.

x	$\Delta x = 0.01$	$\Delta x = 0.001$	$\Delta x = 0.0001$	$\Delta x = 0.00001$
0	0	0	0	0
0.1	1.92908×10^{-5}	1.82556×10^{-6}	1.81536×10^{-7}	1.81411×10^{-8}
0.2	5.47123×10^{-5}	5.38537×10^{-6}	5.37731×10^{-7}	5.37696×10^{-8}
0.3	1.41691×10^{-4}	1.39124×10^{-5}	1.38876×10^{-6}	1.38858×10^{-7}
0.4	2.14233×10^{-4}	2.10649×10^{-5}	2.10301×10^{-6}	2.10275×10^{-7}
0.5	2.63758×10^{-4}	2.59687×10^{-5}	2.59291×10^{-6}	2.59263×10^{-7}
0.6	2.85456×10^{-4}	2.81323×10^{-5}	2.80921×10^{-6}	2.80893×10^{-7}
0.7	2.74873×10^{-4}	2.71086×10^{-5}	2.70717×10^{-6}	2.70695×10^{-7}
0.8	2.27262×10^{-4}	2.24252×10^{-5}	2.23958×10^{-6}	2.23946×10^{-7}
0.9	1.37481×10^{-4}	1.35716×10^{-5}	1.35544×10^{-6}	1.35542×10^{-7}
1	4.59591×10^{-13}	7.58327×10^{-13}	7.92597×10^{-13}	7.22817×10^{-13}

Table 6: Comparison of numerical results for test problem 6 with $u_5^*(x)$ (the fifth iteration of approximated solution in [40]), in different number of nodal points for various Δx.

5. Conclusions

We introduce a practical algorithmic method for studying existence and multiplicity, and also obtain numerical approximations of all branches of solutions for nonlinear boundary value problems, which may be successful in cases where purely analytic methods have failed. Combination of two useful and practical methods, group preserving scheme and shooting method provide us a powerful method. The implementation of the proposed method is simple and speed computation and accuracy are high. The method is implemented successfully for six examples of nonlinear second and third order, two and three point boundary value problems. Interesting results presented in the examples demonstrate the power of the method in searching for multiple solutions as well as the computational efficiency of the method.

Acknowledgments

The authors are grateful to anonymous reviewers for carefully reading this paper and for their comments and suggestions which have improved the paper.

References

[1] S. Abbasbandy, B. Azarnavid, M. S. Alhuthali, *A shooting reproducing kernel Hilbert space method for multiple solutions of nonlinear boundary value problems*, J. Comput. Appl. Math. 279 (2015) 293–305.

[2] S. Abbasbandy, E. Shivanian, *Prediction of multiplicity of solutions of nonlinear boundary value problems: Novel application of homotopy analysis method*, Commun. Nonlinear Sci. Numer. Simulat. 15 (2010) 3830–3846.

[3] S.J. Liao, *A new branch of solutions of boundary–layer flows over a permeable stretching plate*, Int. J. Nonlinear Mech. 42 (2007) 819–830.

[4] H. Xu, S.J. Liao, *Dual solutions of boundary layer flow over an upstream moving plate*, Commun. Nonlinear Sci. Numer. Simulat. 13 (2008) 350–358.

[5] C.-S. Liu, *Cone of non-linear dynamical system and group preserving schemes*, Int. J. Non–Linear Mech. 36 (2001) 1047–1068.

[6] H.-C. Lee, C.-K. Chen, C.-I. Hung, *A modified group–preserving scheme for solving the initial value problems of stiff ordinary differential equations*, Appl. Math. Comput. 133 (2002) 445–459.

[7] C.-S. Liu, *Two–dimensional bilinear oscillator: group–preserving scheme and steady–state motion under harmonic loading*, Int. J. Non–Linear Mech. 38 (2003) 1581–1602.

[8] C.-S. Liu, *Group preserving scheme for backward heat conduction problems*, Int. J. Heat Mass Tran. 47 (2004) 2567–2576.
[9] S.-Y. Zhang, Z.-C. Deng, *Group preserving schemes for nonlinear dynamic system based on RKMK methods*, Appl. Math. Comput. 175 (2006) 497–507.
[10] C.-S. Liu, *New Integrating Methods for Time–Varying Linear Systems and Lie–Group Computations*, CMES, 20 (2007) 157–175.
[11] C.-S. Liu, *Solving an Inverse Sturm–Liouville Problem by a Lie–Group Method*, Bound. Value Prob. 2008 (2008) 18 pages.
[12] S. Abbasbandy, M.S. Hashemi, *Group preserving scheme for the Cauchy problem of the Laplace equation*, Engin. Anal. Bound. Elem. 35 (2011) 1003–1009.
[13] C.-S. Liu, C.-W. Chang, *A novel mixed group preserving scheme for the inverse Cauchy problem of elliptic equations in annular domains*, Engin. Anal. Bound. Elem. 36 (2012) 211–219.
[14] C.-S. Liu, S.N. Atluri, *A $GL(n,\mathbb{R})$ Differential Algebraic Equation Method for Numerical Differentiation of Noisy Signal*, CMES, 92 (2013) 213–239.
[15] C.-S. Liu, W.-S. Jhao, *The Second Lie–Group $SOo(n,1)$ Used to Solve Ordinary Differential Equations*, J. Math. Res. 6 (2014) 18–37.
[16] S. Abbasbandy, R.A. Van Gorder, M. Hajiketabi, M. Mesrizadeh, *Existence and numerical simulation of periodic traveling wave solutions to the Casimir equation for the Ito system*, Commun. Nonlinear Sci. Numer. Simulat. 27 (2015) 254–262.
[17] C.-S. Liu, *The Lie-group shooting method for nonlinear two-point boundary value problems exhibiting multiple solutions*, Comput. Model. Eng. Sci. 13 (2006) 149–163.
[18] C.-S. Liu, *Efficient shooting methods for the second order ordinary differential equations*, Comput. Model. Eng. Sci. 15 (2006) 69–86.
[19] C.-S. Liu, *The Lie–group shooting method for singularly perturbed two-point boundary value problems*, Comput. Model. Eng. Sci. 15 (2006) 179–196.
[20] S. Abbasbandy, R.A. Van Gorder, M. Hajiketabi, *The Lie–group Shooting Method for Radial Symmetric Solutions of the Yamabe Equation*, CMES, 104 (2015) 329–351.
[21] S. Abbasbandy, M.S. Hashemi , C.-S. Liu, *The Lie–group shooting method for solving the Bratu equation*, Commun. Nonlinear Sci. Numer. Simulat. 16 (2011) 4238–4249.
[22] C.-S. Liu, *The Lie–group shooting method for solving multi–dimensional nonlinear boundary value problems*, J. Optim. Theory Appl. 152 (2012) 468–495.
[23] C.-S. Liu, *A Lie–group shooting method for computing eigenvalues and eigenfunctions of Sturm–Liouville problems*, Comput. Model. Eng. Sci. 26 (2008) 157–68.
[24] C.W. Chang, J.R. Chang, C.-S. Liu, *The Lie–group shooting method for solving classical Blasius flat plate problem*, Comput. Mat. Cont.7 (2008) 139–153.
[25] C.W. Chang, J.R. Chang, C.-S. Liu, *The Lie–group shooting method for boundary layer equations in fluid mechanics*, J. Hyd. 18 (2006) 103–108.
[26] C.-S. Liu, C.W. Chang, J.R. Chang, *A new shooting method for solving boundary layer equation in fluid mechanics*, Comput. Mod. Engin. Sci. 32 (2008) 1–15.
[27] C.-S. Liu, *The Lie-group shooting method for boundary–layer problems with suction/injection/reverse flow conditions for power law fluids*, Int. J. Non-Linear Mech. 46 (2011) 1001–1008.
[28] C.-S. Liu, *Computing the eigenvalues of the generalized Sturm–Liouville problems based on the Lie-group SL(2,$\mathbb{R}$)*, J. Comput. Appl. Math. 236 (2012) 4547–4560.
[29] C.-S. Liu, *The Lie-group shooting method for solving multi–dimensional nonlinear boundary value problems*, J. Opt. Theo. Appl. 152 (2012) 468–495.
[30] C.-S. Liu, *A Lie-group shooting method for reconstructing a past time-dependent heat source*, Int. J. Heat Mass Tran. 55 (2012) 1773–1781.
[31] C.-S. Liu, *Developing an SL(2,$\mathbb{R}$) Lie-group shooting method for a singular ϕ–Laplacian in a nonlinear ODE*, Communi. Nonlinear Sci. Num. Simu. 18 (2013) 2327–2339.
[32] C.-S. Liu, *An SL (3,$\mathbb{R}$) shooting method for solving the Falkner–Skan boundary layer equation*, Int. Jo Non–Linear Mech. 49 (2013) 145–151.
[33] A.M. Wazwaz, *Adomian decomposition method for a reliable treatment of the Bratu–type equations*, Appl. Math. Comput. 166 (2005) 652–663.
[34] A. Mohsen, L.F. Sedeek, S.A. Mohamed, *New smoother to enhance multigrid–based methods for Bratu problem*, Appl. Math. Comput. 204 (2008) 325–339.
[35] S. Abbasbandy, *Approximate solution for the nonlinear model of diffusion and reaction in porous catalysts by*

means of the homotopy analysis method, Chem. Eng. J. 136 (2008) 144–150.

[36] E. Magyari,*Exact analytical solution of a nonlinear reaction–diffusion model in porous catalysts*, Chem. Eng. J. 143 (2008) 167–171.

[37] Y.P. Sun, S.B. Liu, S. Keith, *Approximate solution for the nonlinear model of diffusion and reaction in porous catalysts by decomposition method*, Chem. Eng. J. 102 (2004) 1–10.

[38] S. Abbasbandy, E. Magyari, E. Shivanian, *The homotopy analysis method for multiple solutions of nonlinear boundary value problems*, Commun. Nonlinear Sci. Numer. Simulat. 14 (2009) 3530–3536.

[39] Q. Yao, *Successive Iteration and Positive Solution for Nonlinear Second–Order Three–Point Boundary Value Problems*, Comput. Math. Appl. 50 (2005) 433–444.

[40] Q.Yao, *Successive iteration of positive solution for a discontinuous third–order boundary value problem*, Comput. Math. Appl. 53 (2007) 741–749.

[41] M. Kubicek, V. Hlavacek, *Numerical Solution of Nonlinear Boundary Value Problems with Applications*, Prentice–Hall, New York, 1983.